Optical Engineering

OpticalEngineering.SPIEDigitalLibrary.org

Long-period gratings in special geometry fibers for high-resolution and selective sensors

Lars Glavind
John Canning
Shaorui Gao
Kevin Cook
Gang-Ding Peng
Yanhua Luo
Bjarne Funch Skipper
Martin Kristensen

SPIE.

Long-period gratings in special geometry fibers for high-resolution and selective sensors

Lars Glavind,[a,b,*] John Canning,[c] Shaorui Gao,[c,d] Kevin Cook,[c] Gang-Ding Peng,[e] Yanhua Luo,[e] Bjarne Funch Skipper,[f] and Martin Kristensen[b]
[a]Technology & Service Solutions, Vestas Wind Systems A/S, Hedeager 42, 8200 Aarhus N, Denmark
[b]Aarhus University, Department of Engineering, Finlandsgade 22, 8200 Aarhus N, Denmark
[c]University of Sydney, School of Chemistry, Interdisciplinary Photonics Laboratories, 222 Madsen Building F09, Sydney, New South Wales 2006, Australia
[d]Zhejiang University, Center for Optical and Electromagnetic Research, Hangzhou 310058, China
[e]University of New South Wales, Photonics and Optical Communications, Sydney, New South Wales 2052, Australia
[f]Aarhus University, Aarhus School of Engineering, Finlandsgade 22, 8200 Aarhus N, Denmark

Abstract. Advantages for sensor applications of long-period gratings (LPGs) in special optical fibers are reported. Two consecutive LPGs separated by 60 to 100 mm interfere to improve the resolution and reduce noise in a highly doped fiber with inner cladding and in a D-shaped fiber. These gratings provide good contrast to increase the resolution for sensing applications, with or without access to the surroundings along the fiber. The mode profiles of the devices were characterized experimentally to gain deeper insight into the improved functionality. [DOI: 10.1117/1.OE.53.6.066109]

Keywords: optics; gratings; fiber optic sensors.

Paper 140170 received Jan. 31, 2014; revised manuscript received May 19, 2014; accepted for publication May 28, 2014; published online Jun. 25, 2014.

1 Introduction

Since the discovery of useful germanosilicate photosensitivity by Hill et al.[1] and with side writing of gratings,[2] there has been rapid development in optical devices utilizing fiber gratings. In particular, fiber Bragg gratings (FBGs) have been utilized in numerous applications as they have narrow bandwidths and are sensitive to strain and temperature. UV-written long-period gratings (LPGs) were demonstrated in optical fibers by Vengsarkar et al.[3] Compared to FBGs, the bandwidth of the LPG resonance is very broad, typically about 20 nm,[4] which results in limited effective resolution for interrogating their resonant dip and shift. However, it is possible to utilize the general principle of interaction between a particle and two consecutive oscillatory fields, developed originally by Ramsey,[5] where identical LPGs in an optical fiber act as a Mach–Zehnder (MZ) device in transmission,[6] which provides narrow resonances for high-resolution detection of the sensing parameter and reduces noise.[5] This principle has been demonstrated for various sensing applications such as refractive index and bends sensing.[7–9] Utilizing this principle in special fibers with and without access along the fiber to the surroundings provides devices for a large number of applications. It has been demonstrated that LPGs are suitable for structural health monitoring, especially for large structures such as wind turbines, as they can provide directional bend sensing of the blades, due to the fiber geometry.[4] These sensors can also provide the possibility for direct compensation of temperature drift. The utilization in D-shaped fibers provides a good access to the surroundings while retaining sufficient robustness; therefore, they are also ideal for several other evanescent field applications.[10,11]

In other areas such as medicine and molecular biology, many optical characterization methods are based on illuminating samples with modulated light for interrogating the phase of a received signal or to obtain information as a function of time. This sometimes involves mechanical methods[12,13] used to control excitation with different mode patterns and extracting delicate information by advanced data processing.[13] One of the limitations is that devices for switching between mode-field patterns are often slow, bulky, and relatively expensive and often limit a practical compact size. A compact and cheap device that can provide switching between different mode patterns can be realized with the MZ configuration in optical fibers. By sweeping the wavelength to tune the phase rather than mechanically moving a cavity, modulation becomes passive (i.e., no moving parts) and faster, resulting in improved noise suppression and longer-term operation.[14]

If the LPGs are inscribed in an optical fiber with an inner cladding (higher RI of the inner part of the cladding), a device is provided that is insensitive to the surroundings, but can be used for sensing at the fiber end where the fiber is cleaved. In such a case, Fresnel reflections can be utilized for interrogation while another sensor function can be operated from the side—such a multiple functionality is the basis of lab-in-a-fiber technologies. Devices based on this principle also have the possibility of being applied to other cases such as input/output in optical storage devices, fundamental physics applications such as generation of doughnut modes for laser cooling and trapping, and launching simple types of Bessel beams.[15]

2 Fabrication and Simulations

LPGs were inscribed in two different silica fibers: a highly B/GeO_2 codoped inner cladding fiber[14,16] (core: [B] ~20 mol.%, [GeO_2] ~33 mol.%; inner cladding: [P] ~11 mol.%, [F] <4 mol.%) and a D-shaped fibee[9] (core: [GeO_2] ~4.5 mol.%, [P_2O_5] ~1 mol.%, both spliced to SMF-28 fiber for launching and collecting the light. In both

*Address all correspondence to: Lars Glavind, E-mail: lagla@vestas.com

cases, the LPGs were inscribed without hydrogen loading. For maximum interference visibility in the lossless case, each of the LPGs should ideally be near 3-dB deep in transmission,[5] such that the power is equally split into the two modes allowing the interferences with 100% visibility.

2.1 *Inner Cladding Fiber*

The step index of the core relative to the outer cladding of the fiber is $\Delta n = 0.005$, the inner cladding is slightly depressed with an average index difference $\Delta n \sim -0.0015$ relative to the outer cladding. Attributable to the higher volatility and diffusivity of fluorine, for the duration of layer deposition, the inner cladding has a sawtooth transverse index-profile with the teeth depth ranging over $\Delta n \sim 0.000$ to -0.002.[14] The cross section is shown in Fig. 1. The index profile for the preform is shown in Fig. 2. This leads to a leaky cladding mode where most of the light lies within the depressed cladding, and the outer part of the intensity pattern oscillates with the index. Such a property makes the fiber sensitive to stress and bending and also sensitive to reflection loss. Therefore, care is necessary when embedding the LPG containing fiber for an application.

In the fiber with inner cladding, a 10-mm-long LPG with a 3-dB resonance dip near 1583 nm was written through an amplitude mask (50:50 duty cycle, $\Lambda = 440\ \mu$m) using the output of an argon fluoride laser (ArF) exciplex laser ($\lambda = 193$ nm, $f_{\text{pulse}} = 200\ \text{mJ/cm}^2$). The second identical LPG was then written 100 mm from the end of the first grating, while its properties in transmission were measured with an erbium ASE source and an optical spectrum analyzer using a resolution of 1 nm.

The fiber was cleaved exactly at the end of the second LPG, and an optical circulator was utilized to interrogate the Fresnel reflection from the cleaved facet. The spectrum is shown in Fig. 3. The dips measuring light lost to the cladding were found to be 14 dB, indicating the imperfect reflection of the cladding mode from the facet but also arising from the fact that these inner cladding modes are lossy and therefore will reduce the MZ fringe contrast.

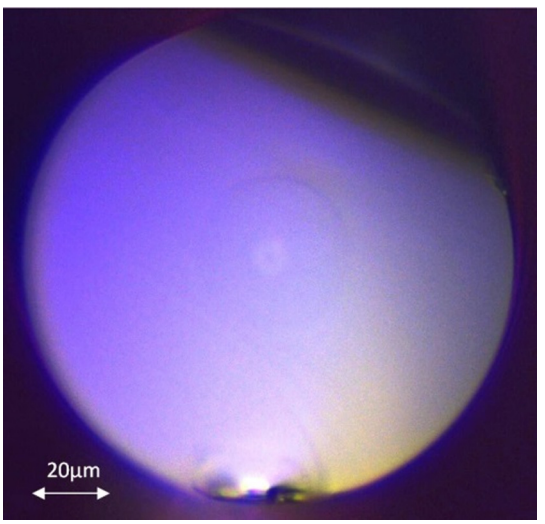

Fig. 1 Cross section of the inner cladding fiber.

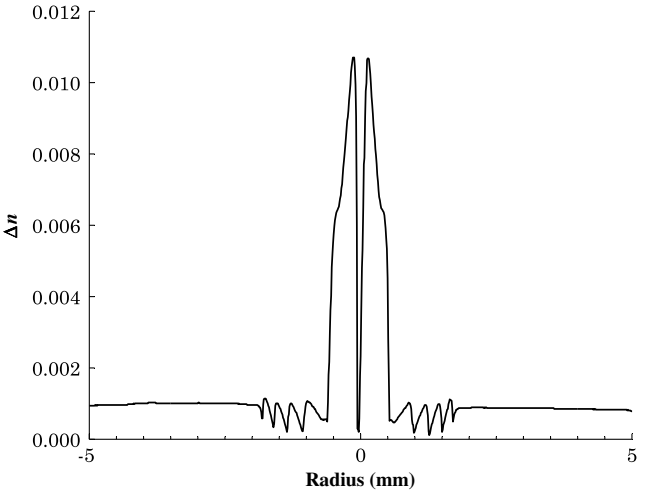

Fig. 2 Index profile of the preform for the inner cladding fiber.

To simulate the distance between the dips in the MZ configuration, the spectra have been modeled utilizing the matrix for transmission gratings as described by[6,17,18]

$$T_i = \begin{bmatrix} \cos(\gamma_c \Delta z) + i\frac{\hat{\sigma}}{\gamma_c}\sin(\gamma_c \Delta z) & i\frac{\kappa}{\gamma_c}\sin(\gamma_c \Delta z) \\ i\frac{\kappa}{\gamma_c}\sin(\gamma_c \Delta z) & \cos(\gamma_c \Delta z) - i\frac{\hat{\sigma}}{\gamma_c}\sin(\gamma_c \Delta z) \end{bmatrix}. \tag{1}$$

For a uniform grating, $\gamma_c \equiv \sqrt{\kappa^2 + \hat{\sigma}^2}$, $\hat{\sigma}$ is a "DC" self-coupling (period-averaged) coupling coefficient, κ is an "AC" cross-coupling coefficient, and Δz is the length of grating.

The transmission spectrum of a composite grating can be found by multiplying each transmission matrix as follows:[19]

$$\begin{bmatrix} F \\ S \end{bmatrix} = T_2 \cdot T_P \cdot T_1 \begin{bmatrix} 1 \\ 0 \end{bmatrix}. \tag{2}$$

The amplitudes of the incident core and cladding modes are here 1 and 0. F and S are the complex amplitudes of the core and cladding modes. T_2 and T_1 are equal, if the gratings are identical. In our case, T_P is the phase shift from the distance between the gratings and is given by

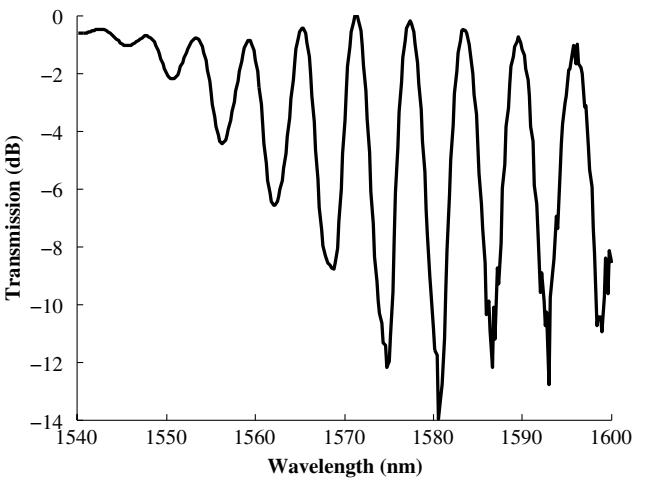

Fig. 3 Normalized spectrum of the Mach–Zehnder (MZ) configuration in the inner cladding fiber.

$$T_{\mathrm{P}} = \begin{bmatrix} \exp\left(i\frac{\Delta\varphi}{2}\right) & 0 \\ 0 & \exp\left(-i\frac{\Delta\varphi}{2}\right) \end{bmatrix}, \tag{3}$$

where $\Delta\varphi = 2\pi\Delta nL/\lambda$, L is the length between the gratings.

From the center wavelength and the grating period, the difference in the effective index for the core and cladding modes can be found[20]

$$\lambda^{(m)} = [n_{\mathrm{eff}} - n_{\mathrm{cl}}^{(m)}]\Lambda, \tag{4}$$

where n_{eff} is the effective index of the guided mode, $n_{\mathrm{cl}}^{(m)}$ is the effective index of an azimuthally symmetric cladding mode of order m, and Λ is the spatial grating period. The asymmetric modes can also, to some smaller degree, be excited even without blazing the grating. For the inner cladding fiber, the center wavelength is $\lambda = 1583$ nm, given $\Delta n_{\mathrm{eff}} \approx 0.0035$.

The simulations of the LPGs in an MZ configuration, with reflection at the cleaved facet of the fiber, are plotted in Fig. 4, where the red line is the reflected power for a single LPG and the black line is the reflected spectra for the two LPGs. Note that loss, especially leaky mode loss, is not included in these simulations. The loss has most influence on small side-lobes and for strong gratings but can affect the fringe contrast obtained as well. Furthermore, the gratings are assumed to be uniform. However, a directly UV-written LPG would always have some minor apodization due to the beam profile of the UV laser. The end-reflections are assumed to be maximum for the core mode and zero for the cladding mode due to the diffraction and a typical small angle on the cleaved end. In addition to all this, Fresnel reflections from the splices and from UV index change during writing are assumed to be negligible and not included in the simulation. As the transverse distribution of the UV-induced changes is unknown, the coupling coefficients are assumed to be 1. The distance between maximum transmission and minimum transmission (core mode) is about 2.8 nm.

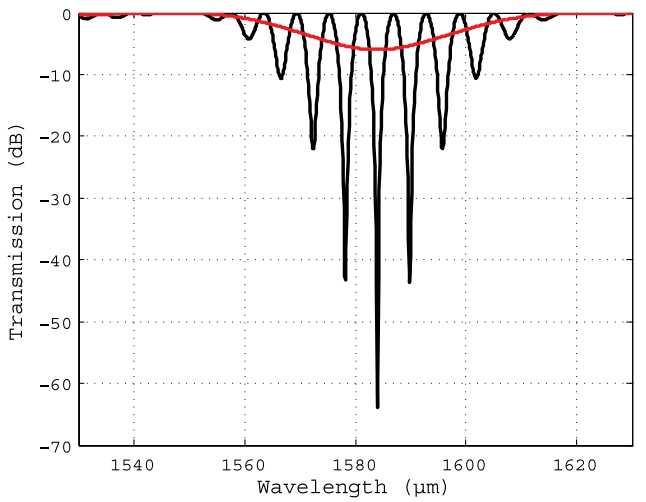

Fig. 4 Normalized spectrum of the model of the long-period grating (LPG) in the inner cladding fiber. The red line is a single 3-dB LPG.

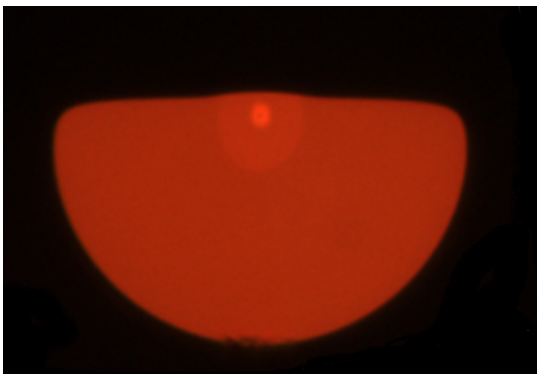

Fig. 5 Cross section of an illuminated D-shaped fiber. The D-shaped fiber also has an inner cladding deposited and visibly seen (fiber diameter of 156 μm).

2.2 *D-Shaped Fiber*

In contrast to the round fiber with inner cladding, a D-shaped fiber provides access to the surroundings along the fiber length. Figure 5 shows the cross section of the D-shaped fiber used in this work. The flat side length is $d \sim 156$ μm and with a distance from the center of the core to the flat side of 8 μm. The index difference of the core and cladding is $\Delta n \sim 0.00456$, and the fiber is single-mode over the 1500-nm range. The mode-field radius is $w \sim 5.4$ μm at 1550 nm. The index profile of the preform, before milling down to a D-shape, is shown in Fig. 6. Note that the fiber has a rise in the cladding near the core. This rise was used to stop crack propagation during the self-assembly of films on D-shaped fibers for lab-in-a-fiber technologies.[21]

In the D-shaped fiber, two identical LPGs were written through an amplitude mask (50:50 duty cycle, $\Lambda = 600$ μm) using the same ArF exciplex laser ($\lambda = 193$ nm) as with the inner cladding fiber. The second identical LPG was written 60 mm from the end of the first grating. As the D-shaped generates form birefringence, and an unpolarized ASE source was used, there are induced polarization-interference ripples visible during writing. The LPGs are therefore written stronger than 3 dB so that they are clearly visible. These LPGs have approximately a 9-dB minimum transmission

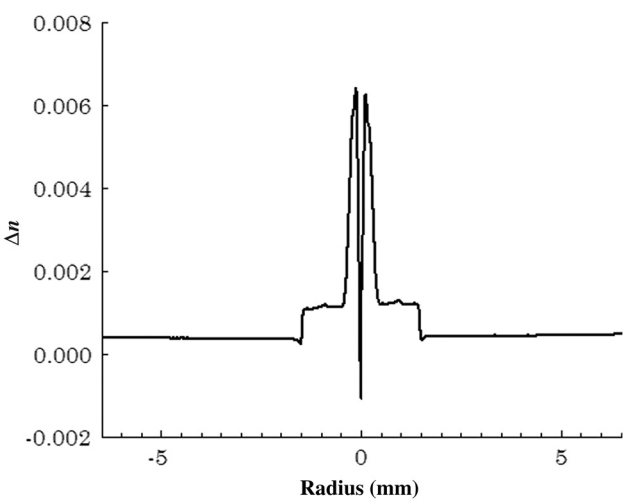

Fig. 6 Index profile of the preform for D-shaped fiber, before milling down to D-shape.

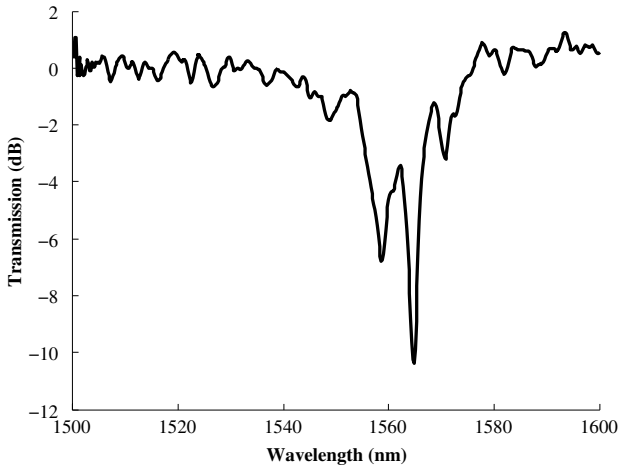

Fig. 7 Normalized spectrum of MZ configuration in the D-shaped fiber (1-nm resolution).

dip centered near 1560 nm. Figure 7 shows the spectrum for the transmission of both LPGs. These were measured using an erbium-doped fiber amplifier (EDFA) and an optical spectrum analyzer (resolution = 1 nm). It is seen that the fringes are still narrow and relatively strong. This device was embedded and utilized as a bend sensor for wind turbines.[9] Additionally, a second LPG device was written, where the center wavelengths of the two LPGs were misaligned—Fig. 8 shows the transmission spectrum of this device, with a dip near 1510 and 1530 nm for the two LPGs, respectively.

The LPGs have been simulated in a similar way as for the inner cladding, shown in Fig. 9, where the red line is the transmitted power for a single LPG and the black line is the spectra for the two LPGs. From Eq. (4), $\Delta n_{\text{eff}} \sim 0.0026$. The lower Δn_{eff} for the D-shaped fiber is due to the core mode lying closer to the cladding/air interface. Note that since the initial LPG is 9 dB, the spectra with the two LPGs will be "over-coupled," affecting the depth of the fringes, but the change in spacing between fringes is small.[22] Furthermore, Fresnel reflections from the splices

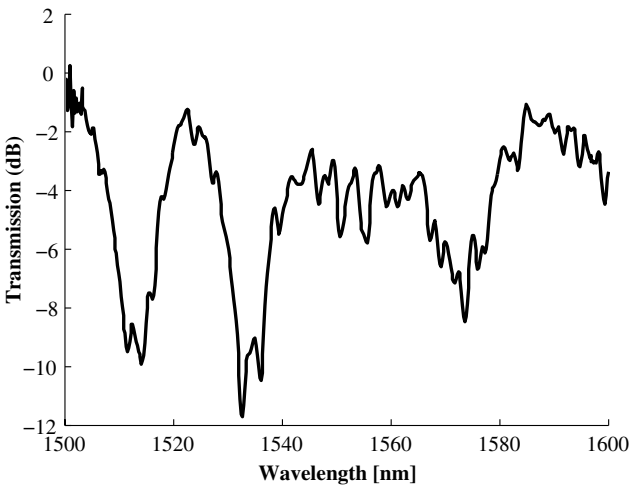

Fig. 8 Normalized spectrum of two LPGs at 1510 and 1530 nm in the D-shaped fiber (1-nm resolution).

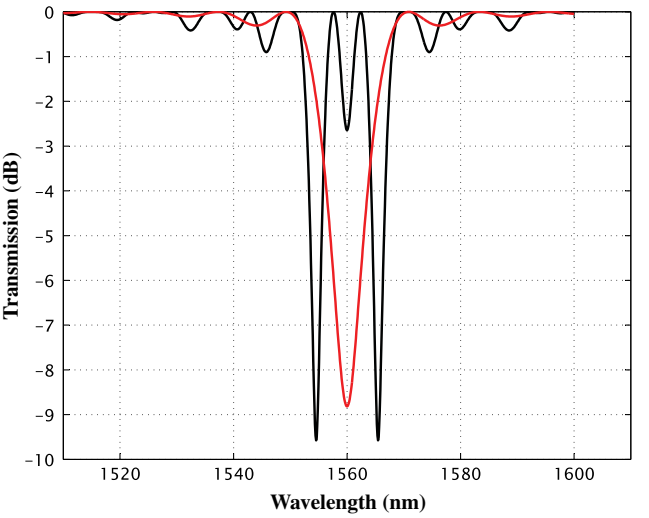

Fig. 9 Normalized spectrum of the model of MZ configuration in the D-shaped fiber. The red line shows the spectrum of a single LPG.

and the UV index change during writing are ignored. The separation between fringes is approximately 6.0 nm for the measured sensor and 5.7 nm for the simulation (influence of birefringence is ignored).

3 Mode Profile Characterization

For mode profile measurements, the fibers were mounted in front of an infrared camera (Vis-NIR vidicon) with a collimation lens (40 × /0.65 NA microscope objective) between the cleaved fiber end and the camera. The mode-field patterns in transmission were measured when launching a 2-mW tuneable laser source (~1550 nm, resolution: 0.1-nm step size, 100-kHz linewidth) into the fibers through the SMF-28 fiber. This is illustrated in Fig. 10.

3.1 *Inner Cladding Fiber*

Figure 11 shows the mode profile, for the inner cladding fiber, at constructive interference between the core and cladding modes corresponding to the maximum back reflection at 1577.4 nm, and Fig. 12 with destructive interference and minimum back reflection at 1580.6 nm (see Fig. 3). The wavelength-shift between exciting predominantly the core and cladding modes is only 3.2 nm. Given the separation is proportional to the effective grating separation, narrower fringes can be used for faster switching between the modes of a given device by increasing the distance between the gratings. Since the cladding modes are confined within the inner cladding, the sensor is immune to the outer cladding surroundings, in contrast to some LPG MZ devices which use cladding modes extending to the outer cladding region.[23] This immunity has been confirmed by applying various liquids on the outside of the fiber without observing any effects.[14]

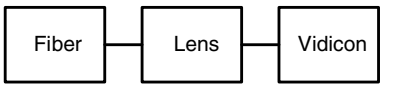

Fig. 10 Schematic of the setup for mode profile measurements.

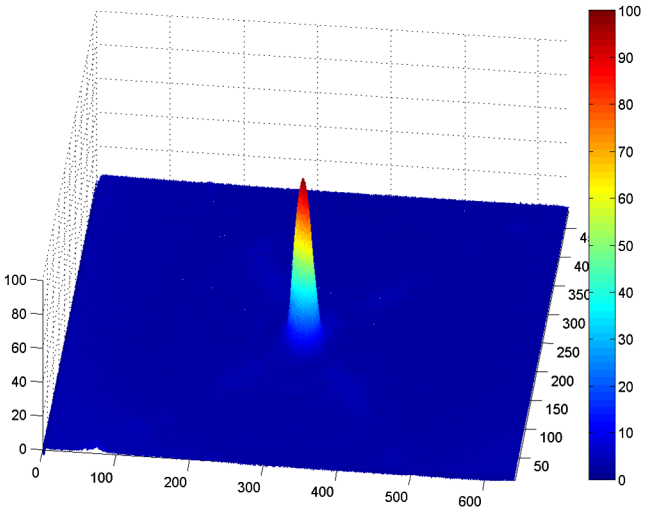

Fig. 11 Mode profile intensity pattern in transmission at 1577.4 nm (core mode).

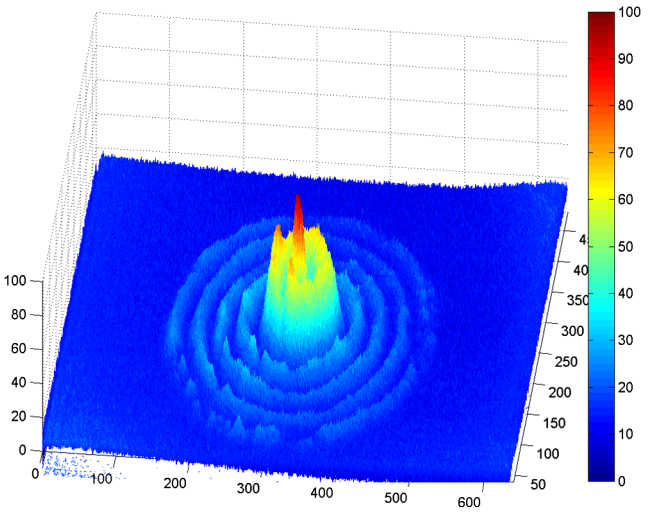

Fig. 12 Mode profile intensity pattern in transmission at 1580.6 nm (cladding mode).

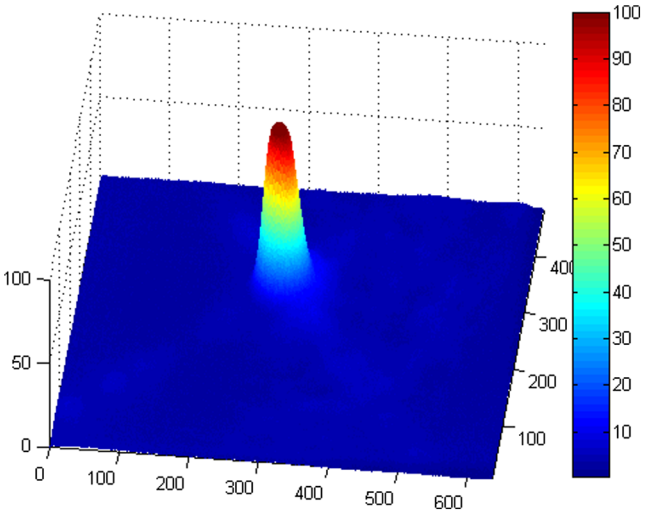

Fig. 13 Mode profile intensity pattern in transmission at 1494.0 nm (core mode).

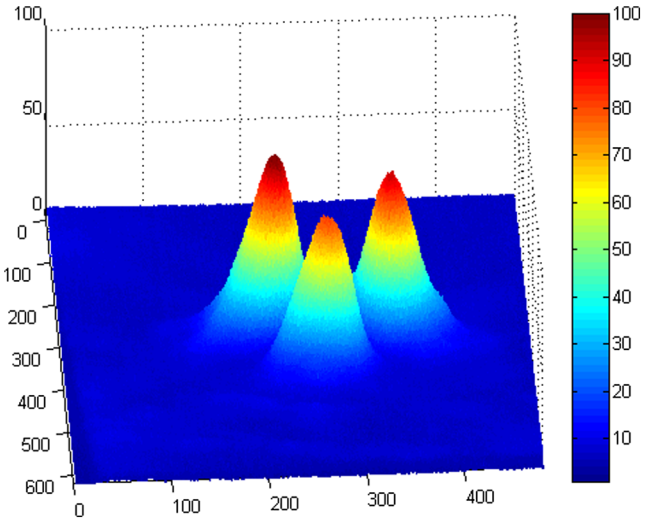

Fig. 14 Mode profile intensity pattern in transmission at 1509.3 nm (cladding mode).

3.2 *D-Shaped Fiber*

For the D-shaped fiber, Figs. 13 and 14 show the mode-field patterns at constructive interference between the core and cladding modes, corresponding to the maximum transmission at 1494.0 nm, and destructive interference and minimum transmission at 1509.3 nm (see Fig. 7).

In the first case, this leads to primarily excitation of the core mode, while in the second case, a cladding mode is excited. Since the two modes have very different patterns, they provide excellent spatial discrimination between effects in the core and cladding, which is ideal for the detection of bending and stress. However, the detailed signal interpretation is complicated by polarization effects and some polarization discrimination is necessary. In addition, they also have different fields overlap with the region outside on the D-flat, which can be used for chemical and biological sensing, for example. The sensitivity to ethanol has been experimentally demonstrated to provide a wavelength shift of about 0.6 nm.

The device in the D-shaped fiber shows only negligible changes with wavelength due to polarization; however, it depends on fiber composition and physical parameters such as the core-center to flat distance. For the sensor to have high birefringence, the distance must be relatively short;[24] however, this would generate loss and even change the mode profiles.

4 Discussion

The mode profiles of the sensors in the two fiber types were characterized experimentally to gain deeper insight into the improved functionality. In general, the two devices have some similarities. They both utilize UV-written LPGs in an MZ configuration to improve the sensitivity. The fringe separation can easily be changed with the distance between the LPGs and thereby optimized for a given application. Compared with a standard LPG in a normal circular fiber, the LPGs in special geometric fibers can provide selectivity to sensing of particular effects and suppress other effects.

Selecting the inner cladding of a fiber provides a very robust device which is immune to the surroundings along the fiber, while enabling a highly sensitive interference device for sensing at the fiber end. On the other hand, the D-shaped fiber, where the interface to the surroundings is very close to the modes in the fiber, provides a device which is highly sensitive to changes in the surroundings. Coupling to the round inner cladding fiber is straightforward, as the fiber dimensions are similar to an SMF-28, whereas the D-shaped fiber requires more care for proper coupling due to the asymmetrical shape.

In the D-shaped fiber, both the core and cladding modes are close to the surface at the flat side, and thereby both modes utilized by the LPG are affected by the coating index, or in the case of naked fiber, the surrounding index. This is different from the inner cladding fiber, where neither core nor cladding modes used by an LPG are affected, and conventional fiber LPGs where the core mode is not affected although the cladding mode will be. This provides the possibility of measurement using both modes, and utilizing one as an internal reference, potentially reducing noise and providing improved spectral resolution and/or selectivity. The D-shaped fiber sensor is, therefore, particularly suitable for a chemical or biological sensor. However, as both modes are close to the flat side, the fiber-sensor is birefringent. This must be taken into consideration for a given application, where it needs to be controlled and/or exploited. With appropriate recoating, the D-shaped fiber can be protected against the surroundings; this has been recently demonstrated with a low-index coating (refractive index 1.375),[9] although the sensitivity is reduced as the index step to the recoating is smaller than to air. Additionally, the D-shaped fiber LPG sensor can have patterns created on the flat side: e.g., for quasiphase-matched nonlinear processes[11] or grating-assisted couplers. LPGs are sensitive to temperature and strain, which must be taken into consideration for a given application; however, the sensitivity can be suppressed by the fiber and grating composition.[4] For example, considering the D-shaped fiber, the germanium doped core can expand more in one direction compared to a symmetrical fiber affecting the sensitivity to strain and temperature.

Finally, an interesting application of the inner cladding fiber would be to provide improved resolution of a scanning near-field optical microscope (SNOM) or a fluorescence variant of such. By tapering the end of the fiber to work as a lens and simultaneously launching two lasers into the fiber, it is possible to construct low-cost devices such as a very cheap version of subdiffraction resolution fluorescence microscope.[13] This works because one laser line is off-resonance with the grating, providing optical excitation of, for example, a fluorophore, whereas the other laser optically depletes the fluorescence while in resonance with the grating and digitally wavelength-modulated between peak and dip of the interference pattern, providing a simple modulation scheme. The modulation speed could be very high by using a 10- to 40-Gbit/s electro-optical modulator, and thereby allow fast surface scanning with nanometer resolution and simultaneously give access to advanced quantum-optical effects. The primary concern would be the signal strength, but it could be significantly improved compared to a standard SNOM by only tapering the fiber-end moderately down, since subdiffraction resolution is provided by the depletion and pattern-modulation anyway. This kind of passive modulation is also suitable as an alternative method of obtaining high-resolution imaging using dynamic optical coherence tomography where probe movement is necessary,[25] which is not always a desirable approach within a human body.

5 Conclusion

This work demonstrates how sensors based on LPGs acting as MZ interferometers in optical fibers for high resolution and selectivity can be exploited for a number of different applications. Based on the selection of fiber, the device can be either sensitive or insensitive to the surroundings along the fiber and/or provide sensing from the end-face of the fiber. Clear switching between the core and cladding modes in transmission through the device has been demonstrated, opening up a passive approach to spatial modulation. The D-fiber platform also offers potential multiple functionality with one fiber.

Acknowledgments

The authors thank Vestas Wind Systems A/S and Australian Research Council (ARC) grant (FT110100116) for funding. Shaorui Gao thanks China Scholarship Council (CSC) for a scholarship and support under the State Scholarship Fund. The authors also thank the Department of Industry, Innovation, Science, and Research (DIISR), Australia, for support in an International Science Linkages (ISL) project (CG130013) and also the Australian Research Council (ARC) for two LIEF grants (LE0883038 and LE100100098) that helped to establish the National Fiber Facility at UNSW.

References

1. K. O. Hill et al., "Photosensitivity in optical fibre waveguides—application to reflection filter fabrication," *Appl. Phys. Lett.* **32**(10), 647–649 (1978).
2. G. Meltz, W. W. Morey, and W. H. Glenn, "Formation of Bragg gratings in optical fibres by a transverse holographic method," *Opt. Lett.* **14**(15), 823–825 (1989).
3. A. M. Vengsarkar et al., "Long-period fibre gratings as band-rejection filters," *J. Lightwave Technol.* **14**(1), 58–65 (1996).
4. L. Glavind et al., "Fibre-optical grating sensors for wind turbine blades: a review," *Opt. Eng.* **52**(3), 030901 (2013).
5. N. F. Ramsey, *Molecular Beams*, 1st ed., University Press, England (1956).
6. E. Dianov et al., "In-fibre Mach–Zehnder interferometer based on a pair of long-period gratings," in *22nd European Conf. on Optical Communication (ECOC '96)*, Vol. 1, pp. 65–68, IEEE, Oslo, Norway (1996).
7. Z. Tian et al., "Refractive index sensing with Mach–Zehnder interferometer based on concatenating two single-mode fibre tapers," *IEEE Photonics Technol. Lett.* **20**(8), 626–628 (2008).
8. T. Allsop et al., "A high sensitivity refractometer based upon a long period grating Mach–Zehnder interferometer," *Rev. Sci. Instrum.* **73**, 1702–1705 (2002).
9. L. Glavind et al., "Enhanced resolution of long-period grating bend sensor," *Proc. SPIE* **8924**, 892437 (2013).
10. Y. N. Ning et al., "A systematic classification and identification of optical fibre sensors," *Sens. Actuators A* **29**(1), 21–36 (1991).
11. V. Pruneri et al., "Greater than 20%-efficient frequency doubling of 1532-nm nanosecond pulses in quasi-phase-matched germanosilicate optical fibres," *Opt. Lett.* **24**(4), 208–210 (1999).
12. D. D. Sampson, "Human cancer imaging with optical coherence tomography microscope-in-a-needle technology," (Plenary talk) presented at *3rd Asia Pacific Optical Sensors Conference (APOS 2012)*, Sydney, Australia (2012).
13. T. A. Klar and S. W. Hell, "Subdiffraction resolution in far-field fluorescence microscopy," *Opt. Lett.* **24**(14), 954–956 (1999).
14. J. Canning, M. Kristensen, and K. Cook, "Wavelength-selective mode-switching in a reflective long period grating Mach–Zehnder

interferometer," in *Advanced Photonics Congress*, OSA, Colorado Springs, Colorado United States (2012).
15. M. Mirhosseini et al., "Rapid generation of light beams carrying orbital angular momentum," *Opt. Express* **21**(25), 30196–30203 (2013).
16. S. Bandyopadhyay et al., "Ultrahigh-temperature regenerated gratings in boron-codoped germanosilicate optical fibre using 193 nm," *Opt. Lett.* **33**(16), 1917–1919 (2008).
17. T. Erdogan, "Fibre grating spectra," *J. Lightwave Technol.* **15**(8), 1277–1294 (1997).
18. D. Marcuse, "Directional-couplers made of nonidentical asymmetric slabs. 2. Grating-assisted couplers," *J. Lightwave Technol.* **5**(2), 268–273 (1987).
19. Y. Tan et al., "Microfibre Mach–Zehnder interferometer based on long period grating for sensing applications," *Opt. Express* **21**(1), 154–164 (2013).
20. V. Bhatia et al., "Temperature-insensitive and strain-insensitive long-period grating sensors for smart structures," *Opt. Eng.* **36**(7), 1872–1876 (1997).
21. L. Moura et al., "A fluorescence study of self-assembled silica layers on D-shaped optical fibre," *Proc. SPIE* **8924**, 89241V (2013).
22. N. F. Ramsey, "Experiments with separated oscillatory fields and hydrogen masers," *Rev. Mod. Phys.* **62**, 541–552 (1990).
23. O. Duhem, J. F. Henninot, and M. Douay, "Study of in fibre Mach–Zehnder interferometer based on two spaced 3-dB long period gratings surrounded by a refractive index higher than that of silica," *Opt. Commun.* **180**(4–6), 255–262 (2000).
24. D. Marcuse, F. Ladouceur, and J. Love, "Vector modes of D-shaped fibres," *IEE Proc. J. Optoelectron.* **139**(2), 117–126 (1992).
25. D. D. Sampson, "Trends and prospects for optical coherence tomography," *Proc. SPIE* **5502**, 25–32 (2004).

Lars Glavind received his BEng degree in electronics from Engineering College of Aarhus in 2007 and his MS degree in optics and electronics from Aarhus University in 2009. For one year, he worked as a research engineer, with applied research projects, at Vestas Wind Systems A/S. In 2014, he received his PhD degree from Aarhus University, regarding long-period gratings as blade load sensors for wind turbines. Currently, he is working at Vestas Wind Systems A/S.

John Canning runs the Interdisciplinary Photonics Laboratories at the University of Sydney and is conjoint professor at the University of NSW. He has over 600 journals and conference papers across materials, photonics, and devices, has lodged more than 40 patents, and has cofounded several companies as well as offering consulting services in photonics and materials.

Shaorui Gao received his BE degree in optoelectronics from Shandong University, China, in 2009. Currently, he is pursuing his PhD degree at Zhejiang University, China, and visiting the interdisciplinary Photonics Laboratories at the University of Sydney. His research interests include fiber Bragg gratings, fiber lasers, and their applications in sensing and communication.

Kevin Cook obtained his PhD degree in physics from Heriot-Watt University (Edinburgh, Scotland) in 2005, where he studied the nonlinear effects of supercontinuum generation in glasses. From 2006 to 2007, he worked at the University of Bath (Bath, England), where he was involved in the development of photonic crystal fibers and hollow-core photonic bandgap fibers. Currently, he is working as a research fellow at the interdisciplinary Photonics Laboratories, University of Sydney, where his research activities focus on regenerated Bragg gratings for sensing applications as well as self-assembled nanophotonics and surface plasmon sensors.

Gang-Ding Peng received his BSc degree in physics from Fudan University in 1982, and MSc degree in applied physics and PhD degree in electronic engineering from Shanghai Jiao Tong University in 1984 and 1987, respectively. He has been working with UNSW, Australia, since 1991. He is a fellow and life member of both OSA and SPIE. His research interests include optical fibers and devices, fiber sensors, and nonlinear optics.

Yanhua Luo received his BE in polymer material and engineering, and a PhD in polymer chemistry and physics from University of Science and Technology of China in 2004 and 2009, respectively. During these periods, he has visited the University of New South Wales as a visiting student to do research about POF gratings. He does research about photonics materials and has published 54 journal and 30 conference papers. He is working as a lab manager of Photonic and Optical Communications Laboratory at UNSW. He is an OSA member.

Bjarne Funch Skipper received his MS degree in electrical engineering from Aalborg University, Denmark, in 1986. He received an industrial PhD degree in narrow linewidth lasers for coherent optical communication in 1989. He has been involved in research and development of fiber-optic telecommunication systems and now he is with Aarhus School of Engineering in Denmark.

Martin Kristensen is a professor of photonics in the Department of Engineering at Aarhus University. Before this, he spent more than 10 years at the Technical University of Denmark (DTU), where he headed a group specializing in optical fiber and waveguide components. He has much experience in design, fabrication, and characterization of optical components and has published more than 300 scientific journals and conference papers and supervised 28 PhD students. He has participated in five EU research projects.